

Lognormal-mixture dynamics and calibration to market volatility smiles

Damiano Brigo Fabio Mercurio Francesco Rapisarda

Product and Business Development Group
Banca IMI, San Paolo-IMI Group
Corso Matteotti, 6
20121 Milano, Italy
Fax: +39 02 7601 9324

E-mail: brigo@bancaimi.it fmercurio@bancaimi.it frapisarda@bancaimi.it

Abstract

We introduce a general class of analytically tractable models for the dynamics of an asset price based on the assumption that the asset-price density is given by the mixture of known basic densities. We consider the lognormal-mixture model as a fundamental example, deriving explicit dynamics, closed form formulas for option prices and analytical approximations for the implied volatility function. We then introduce the asset-price model that is obtained by shifting the previous lognormal-mixture dynamics and investigate its analytical tractability. We finally consider specific examples of calibration to real market option data.

1 Introduction

As is widely known, the Black and Scholes (1973) model can not consistently price all European options that are quoted in one specific market. The assumption of a constant volatility that should be used to price any derivative security with the same underlying asset fails to hold true in practice.

In real markets, the implied volatility curves typically have skewed or smiley shapes. The term “skew” is used to indicate those structures where low-strikes implied volatilities are higher than high-strikes implied volatilities. The term “smile” is used instead to denote those structures with a minimum value around the underlying forward price.

If, for every fixed maturity, the implied volatilities were equal for different strikes but different along the time-to-maturity dimension, we could use the following simple extension

of the Black-Scholes model to exactly retrieve the market option prices:

$$dS_t = \mu S_t dt + \sigma_t S_t dW_t,$$

where σ_t is a time-dependent (deterministic) volatility function.

However, real financial markets display more complex volatility structures, so that the extended Black-Scholes model does not lead to a satisfactory fitting of market data. This issue can then be tackled by introducing a more articulated form of the volatility coefficient in the stock-price dynamics. This is the approach we follow in this paper. We in fact propose two different stock-price models by specifying the stock price dynamics under a given forward-measure. The volatility σ_t we introduce is in both cases a function of time t and the stock price S_t at the same time. By doing so, we are able to construct two models that lead either to skews or to smiles in the term structure of implied volatilities.

Many researchers have tried to address the problem of a good, possibly exact, fitting of market option data. We now briefly review the major approaches that have been proposed.

A first approach is based on assuming an *alternative explicit dynamics* for the stock-price process that immediately leads to volatility smiles or skews. In general this approach does not provide sufficient flexibility to properly calibrate the whole volatility surface. An example is the general CEV process being analysed by Cox (1975) and Cox and Ross (1976). A general class of processes is due to Carr et al. (1999). The first class of models we propose also fall into this *alternative explicit dynamics* category, and while it adds flexibility with respect to the previous known examples, it does not completely solve the flexibility issue.

A second approach is based on the assumption of a *continuum of traded strikes* and goes back to Breeden and Litzenberger (1978). Successive developments are due, among all, to Dupire (1994, 1997) and Derman and Kani (1994, 1998) who derive an explicit expression for the Black-Scholes volatility as a function of strike and maturity. This approach has the major drawback that one needs to smoothly interpolate option prices between consecutive strikes in order to be able to differentiate them twice with respect to the strike. Explicit expressions for the risk-neutral stock price dynamics are also derived by Avellaneda et al. (1997) by minimizing the relative entropy to a prior distribution, and by Brown and Randall (1999) by assuming a quite flexible analytical function describing the volatility surface.

Another approach, pioneered by Rubinstein (1994), consists of finding the risk-neutral probabilities in a binomial/trinomial model for the stock price that lead to a best fitting of market option prices due to some smoothness criterion. We refer to this approach as to the *lattice* approach. Further examples are in Jackwerth and Rubinstein (1996) and Britten-Jones and Neuberger (1999).

A last approach is given by what we may refer to as *incomplete-market* approach. It includes stochastic-volatility models, such as those of Hull and White (1987), Heston (1993) and Tompkins (2000a, 2000b), and jump-diffusion models, such as that of Prigent, Renault and Scaillet (2000).

In general the problem of finding a risk-neutral distribution that consistently prices all quoted options is largely undetermined. A possible solution is given by assuming a par-

ticular *parametric risk-neutral distribution* depending on several, possibly time-dependent, parameters and then use such parameters for the volatility calibration. An example of this approach is the work by Shimko (1993). But the question remains of finding an asset price dynamics consistent with the chosen parametric form of the risk-neutral density. The models we propose addresses this question by finding a dynamics leading to a parametric risk-neutral distribution that is flexible enough for practical purposes. The resulting process combines therefore the *parametric risk-neutral distribution* approach with the *alternative dynamics approach*, providing explicit dynamics leading to flexible parametric risk-neutral densities.

The major challenge that our models are able to face is the introduction of a forward-measure distribution that leads i) to *analytical formulas* for European options, so that the calibration to market data and the computation of Greeks can be extremely rapid, ii) to *explicit asset-price dynamics*, so that exotic claims can be priced through a Monte Carlo simulation and iii) to *recombining lattices*, so that instruments with early-exercise features can be valued via backward calculation in the tree.

The paper is structured as follows. Section 2 proposes a general class of asset-price models based on marginal densities that are given by the mixture of some basic densities. Section 3 considers the particular case of a mixture of lognormal densities and derives closed form formulas for option prices and analytical approximations for the implied volatility function. Section 4 introduces the asset-price model that is obtained by shifting the previous lognormal-mixture dynamics and investigate its analytical tractability. Section 5 considers specific examples of calibration to real market option data. Section 6 concludes the paper.

2 A class of analytical models based on a given mixture of densities

We propose a class of analytically tractable models for an asset-price dynamics that are flexible enough to recover a large variety of market volatility structures. The asset under consideration underlies a given option market and, as such, needs not be tradable itself. Indeed, we can think of an exchange rate, a stock index, and even a forward Libor rate, since caps and floors are nothing but options on Libor rates.

The diffusion processes we obtain follow from assuming a particular distribution for the asset price S under a specific measure. Precisely, we fix a time T and denote by $P(0, T)$ the price at time 0 of a zero-coupon bond with maturity T . We then assume that the T -forward risk-adjusted measure Q^T exists and that the marginal density of S under Q^T is equal to the weighted average of the known densities of some given diffusion processes.

The dynamics of the asset price S under the forward measure Q^T is expressed by

$$dS_t = \mu S_t dt + \sigma(t, S_t) S_t dW_t, \quad (1)$$

where μ is a constant, W is a Q^T -standard Brownian motion and σ is a well-behaved deterministic function.

The μ parameter is completely specified by the definition of Q^T . In fact, if the asset is a stock paying a continuous dividend yield q and rates are deterministic, then $\mu = r - q$, where r is the time T (continuously compounded) risk-free rate. If the asset is an exchange rate and rates are deterministic, then $\mu = r - r_f$, where r_f is foreign risk-free rate for the maturity T . If the asset is a forward rate spanning an interval $[T_0, T]$, $T_0 < T$, then $\mu = 0$ due to the martingale property of forward rates under their corresponding measure.

The function σ , which is usually termed *local volatility* in the financial literature, must be chosen so as to grant a unique strong solution to the SDE (1). In particular, we assume that $\sigma(\cdot, \cdot)$ satisfies, for a suitable positive constant L , the linear-growth condition

$$\sigma^2(t, y)y^2 \leq L(1 + y^2) \quad \text{uniformly in } t, \quad (2)$$

which basically ensures existence of a strong solution.

Let us then consider N diffusion processes with dynamics given by

$$dS_t^i = \mu S_t^i dt + v_i(t, S_t^i) dW_t, \quad i = 1, \dots, N, \quad (3)$$

with initial value S_0^i , and where $v_i(t, y)$'s are real functions satisfying regularity conditions to ensure existence and uniqueness of the solution to the SDE (3). In particular we assume that, for suitable positive constants L_i 's, the following linear-growth conditions hold

$$v_i^2(t, y) \leq L_i(1 + y^2) \quad \text{uniformly in } t, \quad i = 1, \dots, N, \quad (4)$$

For each t , we denote by $p_t^i(\cdot)$ the density function of S_t^i , i.e., $p_t^i(y) = d(Q^T\{S_t^i \leq y\})/dy$, where, in particular, $p_0^i(y)$ is the δ -Dirac function centered in S_0^i .

The problem we want to address is the derivation of the local volatility $\sigma(t, S_t)$ such that the Q^T -density of S satisfies

$$p_t(y) := \frac{d}{dy} Q^T\{S_t \leq y\} = \sum_{i=1}^N \lambda_i \frac{d}{dy} Q^T\{S_t^i \leq y\} = \sum_{i=1}^N \lambda_i p_t^i(y), \quad (5)$$

where each S_0^i is set to S_0 , and λ_i 's are strictly positive constants such that $\sum_{i=1}^N \lambda_i = 1$. Indeed, $p_t(\cdot)$ is a proper Q^T -density function since, by definition,

$$\int_0^{+\infty} y p_t(y) dy = \sum_{i=1}^N \lambda_i \int_0^{+\infty} y p_t^i(y) dy = \sum_{i=1}^N \lambda_i S_0 e^{\mu t} = S_0 e^{\mu t}.$$

Applying the Fokker-Planck equation

$$\frac{\partial}{\partial t} p_t(y) = -\frac{\partial}{\partial y} (\mu y p_t(y)) + \frac{1}{2} \frac{\partial^2}{\partial y^2} (\sigma^2(t, y) y^2 p_t(y)),$$

with p_t given by (5), to back out the diffusion coefficient σ , we end up with the following SDE for the asset price under the forward measure Q^T :

$$dS_t = \mu S_t dt + \sqrt{\frac{\sum_{i=1}^N \lambda_i v_i^2(t, S_t) p_t^i(S_t)}{\sum_{i=1}^N \lambda_i S_t^2 p_t^i(S_t)}} S_t dW_t. \quad (6)$$

This SDE, however, must be regarded as defining some candidate dynamics that leads to the marginal density (5). A detailed derivation of (6) is in Brigo and Mercurio (2000a).

Let us now give for granted that the SDE (6) has a unique strong solution. Then, remembering the definition (5), it is straightforward to derive the model option prices in terms of the option prices associated to the basic models (3). Indeed, let us consider a European option with maturity T , strike K and written on the asset. Then, if $\omega = 1$ for a call and $\omega = -1$ for a put, the option value \mathcal{O} at the initial time $t = 0$ is given by

$$\begin{aligned}
\mathcal{O} &= P(0, T) E^T \{ [\omega(S_T - K)]^+ \} \\
&= P(0, T) \int_0^{+\infty} [\omega(y - K)]^+ \sum_{i=1}^N \lambda_i p_T^i(y) dy \\
&= \sum_{i=1}^N \lambda_i P(0, T) \int_0^{+\infty} [\omega(y - K)]^+ p_T^i(y) dy \\
&= \sum_{i=1}^N \lambda_i \mathcal{O}_i,
\end{aligned} \tag{7}$$

where E^T denotes expectation under Q^T and \mathcal{O}_i denotes the option price associated to (3).

Remark 2.1. *The assumption that the asset marginal density is given by a mixture of known basic densities finds now an easy justification. We notice, in fact, that, starting from a general asset-price dynamics, it may be quite problematic to come up with analytical formulas for European options. Here, instead, the use of analytically-tractable densities p^i immediately leads to explicit option prices for the process S . Moreover, the virtually unlimited number of parameters in the asset-price dynamics can be quite helpful in achieving a satisfactory calibration to market data.*

We have seen above that a dynamics leading to a marginal density for the asset price that is the convex combination of basic densities induces the same convex combination among the corresponding option prices. Due to the linearity of the derivative operator, the same convex combination applies also to all option Greeks. In particular this ensures that starting from analytically tractable basic densities one finds a model that preserves the analytical tractability.

3 The mixture-of-lognormals case

Let us now review the particular case considered by Brigo and Mercurio (2000a) where the densities $p_t^i(\cdot)$'s are all lognormal. Precisely, we assume that, for each i ,

$$v_i(t, y) = \sigma_i(t)y, \tag{8}$$

where all σ_i 's are deterministic functions of time that are bounded from above and below by positive constants. Notice that if moreover σ_i 's are continuous and we take a finite

time-horizon, then boundedness from above is automatic, and the only condition to be required explicitly is boundedness from below by a positive constant. Then, the marginal density of S^i conditional on S_0 is given by

$$p_t^i(y) = \frac{1}{yV_i(t)\sqrt{2\pi}} \exp \left\{ -\frac{1}{2V_i^2(t)} \left[\ln \frac{y}{S_0} - \mu t + \frac{1}{2}V_i^2(t) \right]^2 \right\}, \quad (9)$$

$$V_i(t) := \sqrt{\int_0^t \sigma_i^2(u) du}.$$

The case where the risk-neutral density is a mixture of lognormal densities has been originally studied by Ritchey (1990)¹ and subsequently used by Melick and Thomas (1997), Bhupinder (1998) and Guo (1998). However, their works are mainly empirical: They simply assumed such risk-neutral density and then studied the resulting fitting to option data. Brigo and Mercurio (2000a), instead, developed the model from a theoretical point of view and derived the specific asset-price dynamics that implies the chosen distribution.

The reason for considering the basic densities (9) is of course due to their analytical tractability and obvious connection with the Black and Scholes (1973) model. Moreover, as we show in the appendix, the log-returns $\ln(S_t)/\ln(S_0)$, $t > 0$, are more leptokurtic than in the Gaussian case, which may be a nice feature from a practical point of view. Finally, as also reported in the above empirical studies, mixtures of lognormal densities work well in many practical situations, when used to reproduce market volatility structures.

The following result has been proven by Brigo and Mercurio (2000a).

Proposition 3.1. *Let us assume that each σ_i is also continuous and that there exists an $\varepsilon > 0$ such that $\sigma_i(t) = \sigma_0 > 0$, for each t in $[0, \varepsilon]$ and $i = 1, \dots, N$. Then, if we set*

$$\nu(t, y) = \sqrt{\frac{\sum_{i=1}^N \lambda_i \sigma_i^2(t) \frac{1}{V_i(t)} \exp \left\{ -\frac{1}{2V_i^2(t)} \left[\ln \frac{y}{S_0} - \mu t + \frac{1}{2}V_i^2(t) \right]^2 \right\}}{\sum_{i=1}^N \lambda_i \frac{1}{V_i(t)} \exp \left\{ -\frac{1}{2V_i^2(t)} \left[\ln \frac{y}{S_0} - \mu t + \frac{1}{2}V_i^2(t) \right]^2 \right\}}}, \quad (10)$$

for $(t, y) > (0, 0)$ and $\nu(t, y) = \sigma_0$ for $(t, y) = (0, S_0)$, the SDE

$$dS_t = \mu S_t dt + \nu(t, S_t) S_t dW_t, \quad (11)$$

has a unique strong solution whose marginal density is given by the mixture of lognormals

$$p_t(y) = \sum_{i=1}^N \lambda_i \frac{1}{yV_i(t)\sqrt{2\pi}} \exp \left\{ -\frac{1}{2V_i^2(t)} \left[\ln \frac{y}{S_0} - \mu t + \frac{1}{2}V_i^2(t) \right]^2 \right\}. \quad (12)$$

¹Indeed, Ritchey (1990) assumed a mixture of normal densities for the density of the asset log-returns. However, it can be easily shown that this is equivalent to assuming a mixture of lognormal densities for the density of the asset price.

Moreover, for $(t, y) > (0, 0)$, we can write

$$\nu^2(t, y) = \sum_{i=1}^N \Lambda_i(t, y) \sigma_i^2(t), \quad (13)$$

where, for each (t, y) and i , $\Lambda_i(t, y) \geq 0$ and $\sum_{i=1}^N \Lambda_i(t, y) = 1$. As a consequence

$$0 < \tilde{\sigma} \leq \nu(t, y) \leq \hat{\sigma} < +\infty \quad \text{for each } t, y > 0, \quad (14)$$

where

$$\begin{aligned} \tilde{\sigma} &:= \inf_{t \geq 0} \left\{ \min_{i=1, \dots, N} \sigma_i(t) \right\}, \\ \hat{\sigma} &:= \sup_{t \geq 0} \left\{ \max_{i=1, \dots, N} \sigma_i(t) \right\}. \end{aligned}$$

The above proposition provides us with the analytical expression for the diffusion coefficient in the SDE (1) such that the resulting equation has a unique strong solution whose marginal density is given by (5) with p^i 's as in (9). Moreover, the square of the ‘‘local volatility’’ $\nu(t, y)$ can be viewed as a weighted average of the squared ‘‘basic volatilities’’ $\sigma_1^2(t), \dots, \sigma_N^2(t)$, where the weights are all functions of the lognormal marginal densities (9). In particular, the ‘‘local volatility’’ $\nu(t, y)$ lies in the interval $[\tilde{\sigma}, \hat{\sigma}]$.

As we have already noticed, the pricing of European options under the asset-price model (1) with (10) is quite straightforward.² Indeed, we have the following.

Proposition 3.2. *Consider a European option with maturity T , strike K and written on the asset. The option value at the initial time $t = 0$ is then given by the following convex combination of Black-Scholes prices*

$$\mathcal{O} = \omega P(0, T) \sum_{i=1}^N \lambda_i \left[S_0 e^{\mu T} \Phi \left(\omega \frac{\ln \frac{S_0}{K} + (\mu + \frac{1}{2} \eta_i^2) T}{\eta_i \sqrt{T}} \right) - K \Phi \left(\omega \frac{\ln \frac{S_0}{K} + (\mu - \frac{1}{2} \eta_i^2) T}{\eta_i \sqrt{T}} \right) \right], \quad (15)$$

where Φ is the normal cumulative distribution function, $\omega = 1$ for a call and $\omega = -1$ for a put, and

$$\eta_i := \frac{V_i(T)}{\sqrt{T}} = \sqrt{\frac{\int_0^T \sigma_i^2(t) dt}{T}}. \quad (16)$$

The option price (15) leads to smiles in the implied volatility structure. An example of the shape that can be reproduced is shown in Figure 1. Indeed, the volatility implied by the option prices (15) has a minimum exactly at a strike equal to the forward asset price $S_0 e^{\mu T}$. Given the above analytical tractability, we can easily derive an explicit approximation for

²We need also to remark that, under deterministic interest rates, we can actually prove the existence of a unique risk-neutral measure, and hence forward measure.

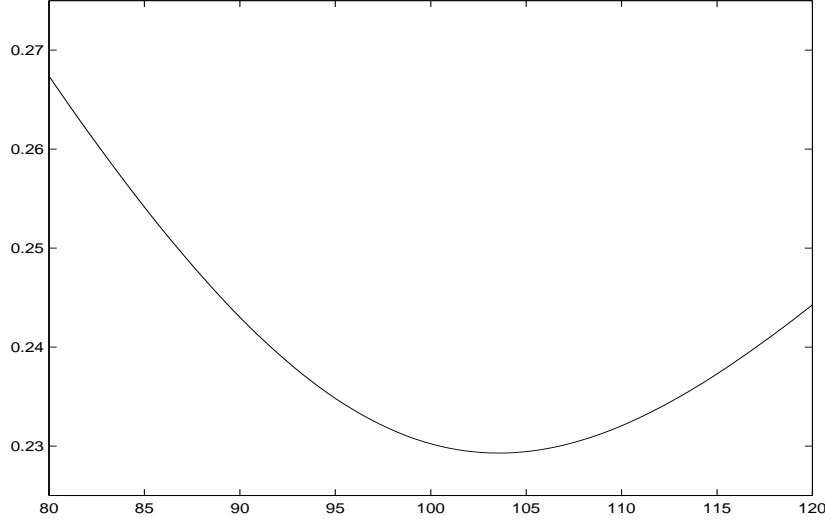


Figure 1: Volatility structure implied by the option prices (15), where we set $\mu = r = 0.035$, $T = 1$, $N = 3$, $(\sigma_1, \sigma_2, \sigma_3) = (0.5, 0.1, 0.2)$, $(\lambda_1, \lambda_2, \lambda_3) = (0.2, 0.3, 0.5)$ and $S_0 = 100$.

the implied volatility as function of the option strike price. More precisely, defining the moneyness m as

$$m := \ln \frac{S_0}{K} + \mu T,$$

the Black-Scholes volatility that, for the given maturity T , is implied by the price (15) is the function $\hat{\sigma}(m)$ that is implicitly defined by the equation

$$\begin{aligned} P(0, T)S_0e^{\mu T} & \left[\Phi\left(\frac{m + \frac{1}{2}\hat{\sigma}(m)^2T}{\hat{\sigma}(m)\sqrt{T}}\right) - e^{-m}\Phi\left(\frac{m - \frac{1}{2}\hat{\sigma}(m)^2T}{\hat{\sigma}(m)\sqrt{T}}\right) \right] \\ & = P(0, T)S_0e^{\mu T} \sum_{i=1}^N \lambda_i \left[\Phi\left(\frac{m + \frac{1}{2}\eta_i^2T}{\eta_i\sqrt{T}}\right) - e^{-m}\Phi\left(\frac{m - \frac{1}{2}\eta_i^2T}{\eta_i\sqrt{T}}\right) \right]. \end{aligned} \quad (17)$$

Proposition 3.3. *The Black-Scholes volatility that is implied by the price (15) is given by*

$$\hat{\sigma}(m) = \hat{\sigma}(0) + \frac{1}{2\hat{\sigma}(0)T} \sum_{i=1}^N \lambda_i \left[\frac{\hat{\sigma}(0)}{\eta_i} e^{\frac{1}{8}(\hat{\sigma}(0)^2 - \eta_i^2)T} - 1 \right] m^2 + o(m^2), \quad (18)$$

where $\hat{\sigma}(0)$ is the ATM-forward implied volatility, which is given by

$$\hat{\sigma}(0) = \frac{2}{\sqrt{T}} \Phi^{-1} \left(\sum_{i=1}^N \lambda_i \Phi \left(\frac{1}{2} \eta_i \sqrt{T} \right) \right). \quad (19)$$

Proof. The expression (18) is nothing but the second-order Taylor expansion of the function $\hat{\sigma}$ around 0, with the first and second derivatives in 0 that are calculated through repeated application of Dini's implicit function theorem. Some algebra then shows that the first derivative in 0 is null and that (19) follows from (17). \square

The model (11) is quite appealing when pricing exotic derivatives. Notice, indeed, that having explicit dynamics implies that the asset-price paths can be simulated by discretising the associated SDE with a numerical scheme. Hence we can use Monte Carlo procedures to price path-dependent derivatives. Claims with early-exercise features can be priced with grids or lattices that can be constructed given the explicit form of the asset-price dynamics.

4 Shifting the overall distribution

We now show how to construct an even more general model by shifting the process (11), while preserving the correct drift. Precisely, we assume that the new asset-price process A is obtained through the following affine transformation of the process S :

$$A_t = A_0 \alpha e^{\mu t} + S_t, \quad (20)$$

where α is a real constant.³ By Ito's formula, we immediately obtain that the asset-price A evolves according to

$$dA_t = \mu A_t dt + \nu(t, A_t - A_0 \alpha e^{\mu t}) (A_t - A_0 \alpha e^{\mu t}) dW_t, \quad (21)$$

where ν is defined by (10).

Some examples of the shapes that can be obtained for the density of A_t are shown in Figure 2 for different values of the parameter α .

The model (21) for the asset price process preserves the analytical tractability of the original process S . Indeed, the price at time 0 of a European call option with strike K , maturity T and written on the asset is

$$\begin{aligned} P(0, T) E^T \{(A_T - K)^+\} &= P(0, T) E^T \{(A_0 \alpha e^{\mu T} + S_T - K)^+\} \\ &= P(0, T) E^T \{(S_T - [K - A_0 \alpha e^{\mu T}])^+\} \end{aligned} \quad (22)$$

Proposition 4.1. *Assuming that $K - A_0 \alpha e^{\mu T} > 0$, the option price can be explicitly written as*

$$\mathcal{O} = \omega P(0, T) \sum_{i=1}^N \lambda_i \left[\mathcal{A}_0 e^{\mu T} \Phi \left(\omega \frac{\ln \frac{\mathcal{A}_0}{\mathcal{K}} + (\mu + \frac{1}{2} \eta_i^2) T}{\eta_i \sqrt{T}} \right) - \mathcal{K} \Phi \left(\omega \frac{\ln \frac{\mathcal{A}_0}{\mathcal{K}} + (\mu - \frac{1}{2} \eta_i^2) T}{\eta_i \sqrt{T}} \right) \right], \quad (23)$$

³It is easy to prove that this is actually the most general affine transformation for which the drift rate of A is μ .

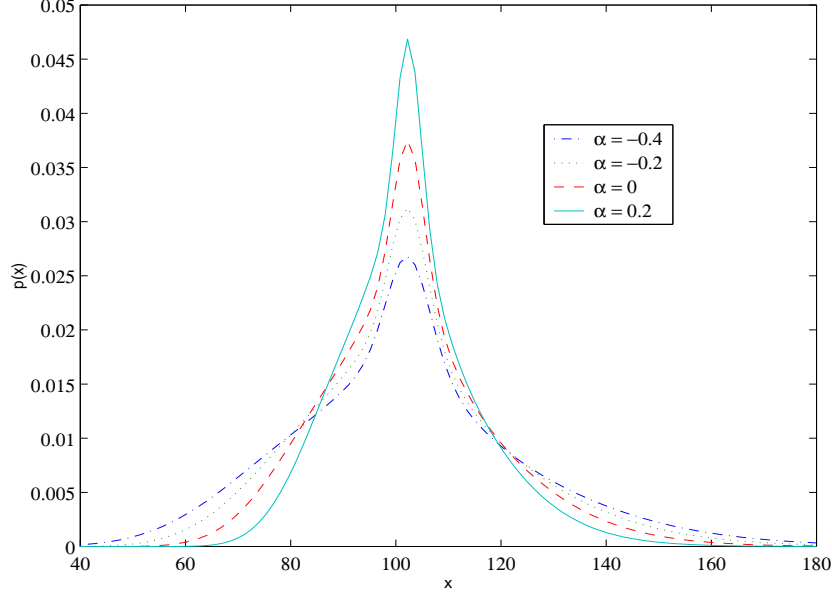


Figure 2: The density function $p(x)$ of A_T for the different values of $\alpha \in \{-0.4, -0.2, 0, 0.2\}$, where we set $A_0 = 100$, $\mu = 0.05$, $T = 0.5$, $N = 3$, $(\eta_1(T), \eta_2(T), \eta_3(T)) = (0.25, 0.09, 0.04)$ and $(\lambda_1, \lambda_2, \lambda_3) = (0.8, 0.1, 0.1)$.

where $\mathcal{K} = K - A_0\alpha e^{\mu T}$, $\mathcal{A}_0 = A_0(1 - \alpha)$, $\omega = 1$ for a call and $\omega = -1$ for a put. Moreover, the Black-Scholes volatility that is implied by the price (23) is given by

$$\begin{aligned} \hat{\sigma}(m) = \hat{\sigma}(0) + \alpha \frac{\sum_{i=1}^N \lambda_i \Phi\left(-\frac{1}{2}\eta_i\sqrt{T}\right) - \frac{1}{2}}{\frac{\sqrt{T}}{\sqrt{2\pi}} e^{-\frac{1}{8}\hat{\sigma}(0)^2 T}} m + \frac{1}{2} \left[\frac{1}{T(1-\alpha)} \sum_{i=1}^N \frac{\lambda_i}{\eta_i} e^{\frac{1}{8}(\hat{\sigma}(0)^2 - \eta_i^2)T} \right. \\ \left. - \frac{1}{\hat{\sigma}(0)T} + \frac{\alpha^2}{4} \hat{\sigma}(0)T \left(\frac{\sum_{i=1}^N \lambda_i \Phi\left(-\frac{1}{2}\eta_i\sqrt{T}\right) - \frac{1}{2}}{\frac{\sqrt{T}}{\sqrt{2\pi}} e^{-\frac{1}{8}\hat{\sigma}(0)^2 T}} \right)^2 \right] m^2 + o(m^2) \end{aligned} \quad (24)$$

where $\hat{\sigma}(0)$ is the ATM-forward implied volatility, which is now given by

$$\hat{\sigma}(0) = \frac{2}{\sqrt{T}} \Phi^{-1} \left((1 - \alpha) \sum_{i=1}^N \lambda_i \Phi\left(\frac{1}{2}\eta_i\sqrt{T}\right) + \frac{\alpha}{2} \right). \quad (25)$$

Proof. The option price (23) immediately follows from (22) remembering (15). The expression (24) is the second-order Taylor expansion of the function $\hat{\sigma}$ around 0, with the first and second derivatives in 0 that are derived, after lengthy calculations, by means of Dini's implicit function theorem. The implied volatility (25) follows instead from the obvious generalization of (17) to the case where the option price is (23). \square

We remark that for $\alpha = 0$ the process A obviously coincides with S while preserving the correct drift. The introduction of this new parameter has the effect that, decreasing α , the

variance of the asset-price at each time increases while maintaining the correct expectation. See also Figure 2 for related examples. Indeed,

$$E(A_t) = A_0 e^{\mu t}$$

$$\text{Var}(A_t) = A_0^2 (1 - \alpha)^2 e^{2\mu t} \left(\sum_{i=1}^N \lambda_i e^{V_i^2(t)} - 1 \right).$$

The parameter α affects the shape of the implied volatility surface in a twofold manner. First, it concurs to determine the level of such surface in that changing α leads to an almost parallel shift of the surface. Second, it moves the strike where the volatility is minimum. Precisely, if $\alpha > 0$ (< 0) the minimum is attained for strikes lower (higher) than the ATM forward price. For related examples, we refer to Figure 3.

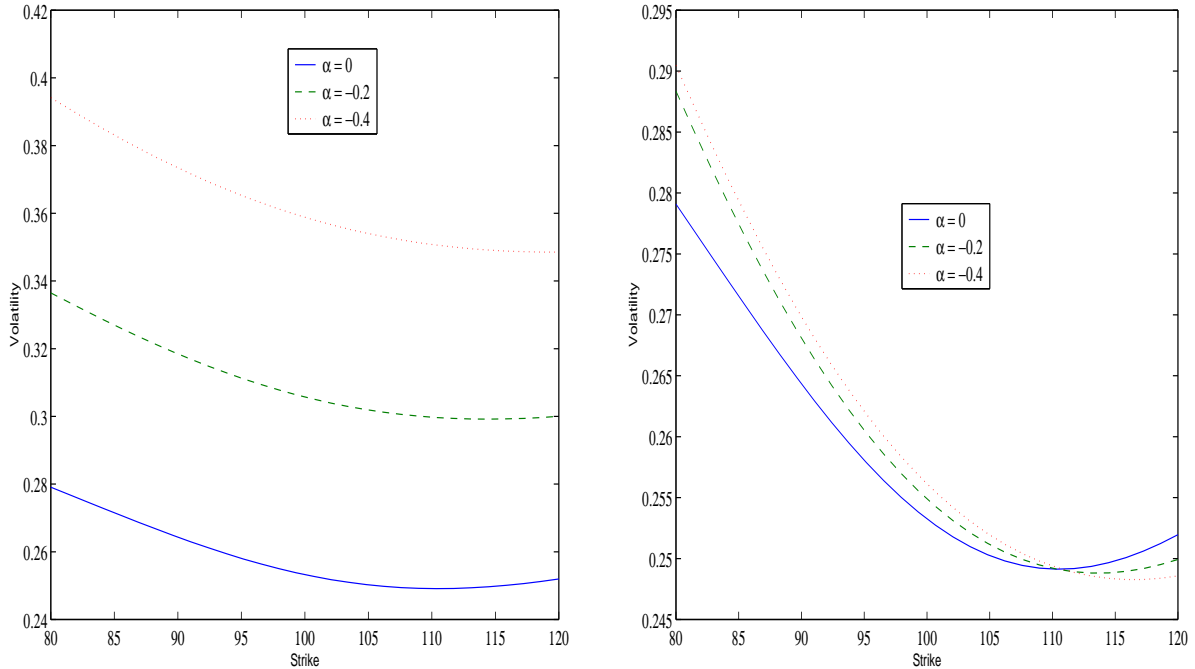


Figure 3: Influence of α on implied volatility curves. Left: implied volatility curve for $A_0 = 100$, $\mu = 0.05$, $N = 2$, $T = 2$, $(\eta_1(T), \eta_2(T)) = (0.35, 0.1)$, $(\lambda_1, \lambda_2) = (0.6, 0.4)$, $\alpha \in \{0, -0.2, -0.4\}$, $K \in [80, 120]$; Right: implied volatility curve for $A_0 = 100$, $\mu = 0.05$, $N = 2$, $T = 2$, $(\lambda_1, \lambda_2) = (0.6, 0.4)$, $K \in [80, 120]$ in the three cases: a) $(\eta_1(T), \eta_2(T)) = (0.35, 0.1)$, $\alpha = 0$; b) $(\eta_1(T), \eta_2(T)) = (0.1099, 0.3553)$, $\alpha = -0.2$; c) $(\eta_1(T), \eta_2(T)) = (0.09809, 0.2979)$, $\alpha = -0.4$;

A large variety of skews for the implied volatility surface can be thus obtained. An example of the volatility surface that is implied by the above option prices is displayed in Figure 4. Notice, indeed, that one can easily find some σ_i 's, satisfying our technical assumptions, that are consistent with the chosen η_i 's. Retrieving such σ_i 's is fundamental

for the discretization of the asset price dynamics one needs to consider in order to price exotic claims.

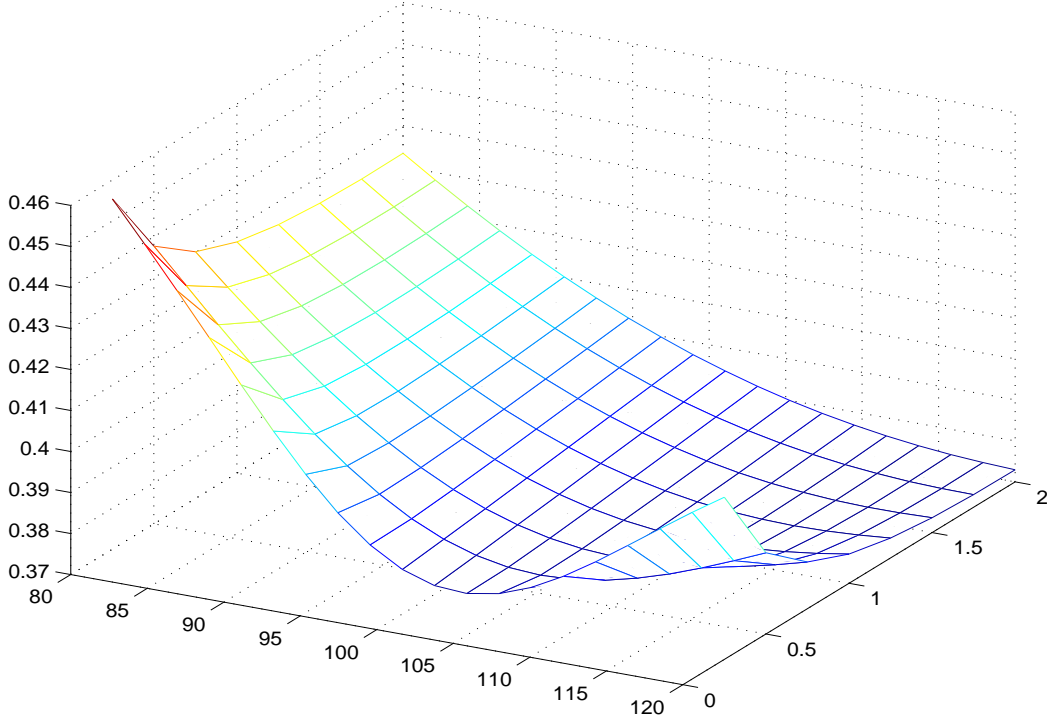


Figure 4: Implied volatility surface for $A_0 = 100$, $\mu = r = 0.05$, $N = 2$, $\mathcal{T} := \{0.25, 0.5, 0.75, 1, 1.25, 1.5, 1.75, 2\}$, $(\eta_1(t), \eta_2(t)) = (0.35, 0.1)$, for each $t \in \mathcal{T}$, $(\lambda_1, \lambda_2) = (0.6, 0.4)$, $\alpha = -0.5$ and T varying in \mathcal{T} .

The explicit option price (23) immediately leads to closed form formulas for the option Greeks as well, since differentiating a linear combination yields the linear combination of the single derivatives. For instance, the option Delta is easily computed as

$$\sum_{i=1}^N \lambda_i P(0, T) e^{\mu T} \left[(1 - \alpha) \Phi(d_1(A_0(1 - \alpha), K - \alpha A_0 e^{\mu T}, T, \mu, \eta_i(T))) - \alpha \Phi(d_2) \right],$$

$$d_{1,2}(S, K, T, \mu, V) = \frac{\ln(S/K) + (\mu \pm V^2/2)T}{V\sqrt{T}},$$

where d_2 's arguments are the same as d_1 's and have been omitted for brevity. Notice that for $\alpha = 0$ this is just a linear combination of Black and Scholes Δ 's.

4.1 Shifting each basic distribution

In order to achieve greater flexibility when trying to reproduce various volatility structures, a possible extension of the model may consist in allowing each density p_t^i to be shifted

independently.

Assuming the dynamics

$$\begin{cases} S_t^i = \beta_i e^{\mu t} + X_t^i \\ dX_t^i = \mu X_t^i dt + \sigma_i(t) X_t^i dW_t \end{cases} \quad (26)$$

which leads to

$$dS_t^i = \mu S_t^i dt + \sigma_i(t) (S_t^i - \beta_i e^{\mu t}) dW_t, \quad (27)$$

we get the natural extension to Eq. (9)

$$p_t^i(y) = \frac{1}{(y - \beta_i e^{\mu t}) V_i(t) \sqrt{2\pi}} \exp \left[-\frac{1}{2V_i^2(t)} \left(\ln \left(\frac{y - \beta_i e^{\mu t}}{S_0 - \beta_i} \right) - \mu t + \frac{1}{2} V_i^2(t) \right)^2 \right], y \geq \beta_i e^{\mu t} \quad (28)$$

and the resulting dynamics for S_t is

$$dS_t = \mu S_t dt + \sqrt{\frac{\sum_{i=1}^n \lambda_i \sigma_i^2(t) (S_t - \beta_i e^{\mu t})^2 p_t^i(S_t)}{\sum_{i=1}^n \lambda_i p_t^i(S_t)}} dW_t \quad (29)$$

Eq. (23) is trivially extended to deal with individual shifts in the basis densities. It is still to be verified that under the assumption of Eq. (26) the corresponding SDE for S_t has a unique strong solution.

5 Applying the models in practice

We now briefly illustrate how to apply our previous models to the three fundamental markets we consider: equity, exchange rate and interest rate markets.

If the asset is a stock or an index paying a continuous dividend yield q , we can assume that interest rates are constant for all maturities and all equal to $r > 0$. Then every forward measure coincides with the (assumed unique) risk-neutral measure, which has $B(t) = e^{rt}$ as numeraire, and the stock/index price dynamics, under such measure, is given by (21) where we put $\mu = r - q$. If the stock/index pays known discrete dividends, the general methodology described by Musiela and Rutkowski (1998) can be applied. In this case, (21) with $\mu = r$ defines the continuous part of the price dynamics and the option price formula (23) holds as long as A_0 is reduced by the present value of all future dividends. As to the calibration to real market data, the pronounced skews that are commonly displayed in stock/index markets can be retrieved by suitably playing with the parameters, especially α (in the case of a common shift for the whole distribution) or the individual β_i 's (for the most general case treated in Section 4.1) which may assume highly negative values. However, reproducing highly steep curves for very short maturities may be still problematic.

Suppose instead that the asset is a forward Libor rate. The forward Libor rate at time t for the period that goes from expiry S to maturity T is defined by

$$F(t, S, T) = \frac{1}{\tau(S, T)} \left[\frac{P(t, S)}{P(t, T)} - 1 \right],$$

where $\tau(S, T)$ is the year fraction from S to T . This is the fundamental quantity that is modelled in the celebrated Libor market models for interest rates. The forward rate dynamics we propose are then given by (21) where we put $\mu = 0$, since $F(\cdot, S, T)$ is a martingale under the forward measure Q^T . Similarly to the equity market, also in the interest rate market pronounced skews are often displayed. Once again the parameter α plays a fundamental role in the calibration to market data.

5.1 The calibration to market data

The virtually unlimited number of parameters can render the model calibration to real market data extremely accurate. However, when solving the optimization problem consisting in minimizing the “distance” between model and market prices according to some favorite criterion, the search for a global minimum can be quite cumbersome and inevitably slow. Suppose you have 10 parameters and just 4 possible values for each of them. This implies that more than one million different combinations of parameter values, hence objective function valuations, are considered. The use of a local-search algorithm can actually speed up the calibration process. However, these algorithms usually provide quite different answers according to the initial guess on the parameter values. In practice, therefore, it is advisable to use a global search algorithm with few model parameters and then refine the search with a local algorithm around the last solution being found.

Let us assume we have M option maturities $T_1 < T_2 < \dots < T_M$. We set $v_{i,j} := \eta_i(T_j)$ for $i = 1, \dots, N$ and $j = 1, \dots, M$. The option price (23) only implicitly depends on the functions σ_i 's since the quantities that directly affect it are the $v_{i,j}$'s. The model calibration, therefore, must be performed on these variables. The set of constraints $v_{i,j+1} > v_{i,j} \sqrt{T_j/T_{j+1}}$, for each i and j , must be then introduced to avoid imaginary values for the functions σ_i 's. An additional constraint is on the parameter α , which must satisfy the condition $K > A_0 \alpha e^{\mu T}$ for each traded strike K .

To reduce the number of parameters we may assume that no changes occur along the maturity dimension by setting $v_{i,j} = \bar{v}_i > 0$, which is always consistent with some admissible σ_i 's. The fitting quality however may worsen considerably. The choice made in one of the following examples (calibrated on EUR/USD market data) is instead to greatly reduce the number of fitting parameters by specifying a given parametric form for functions $\eta_i(t)$. This form is parsimonious but still flexible enough to achieve a very good fitting quality.

As to the number of lognormal densities to choose, it is enough to set $N = 2$ or $N = 3$ in most practical applications.

5.2 An example of calibration

The fitting quality of the extended model (20) has been first investigated by Brigo and Mercurio (2000b) through market data of the Italian MIB30 equity index. We here consider a different example based on interest rates volatility data. Precisely, we use the caplet volatilities that are stripped from the quoted in-the-money and out-of-the-money Euro

cap/floor volatilities as of November 14th, 2000. We focus on the volatilities of the two-year caplets with the underlying Libor rate resetting at 1.5 years. The underlying forward rate is 5.32%, the considered strikes are 4%, 4.25%, 4.5%, 4.75%, 5%, 5.25%, 5.5%, 5.75%, 6%, 6.25%, 6.5% and the associated (mid) volatilities are 15.22%, 15.14%, 15.10%, 15.08%, 15.09%, 15.12%, 15.17%, 15.28%, 15.40%, 15.52%, 15.69%.

Setting $N = 2$ (the index density is a mixture of two lognormal densities), $v_i := \eta_i(1.5)$, $i = 1, 2$, and $\lambda_2 = 1 - \lambda_1$, we looked for the admissible values of λ_1 , v_1 , v_2 and α minimizing the squared percentage difference between model and market (mid) prices. We obtained $\lambda_1 = 0.2412$, $\lambda_2 = 0.7588$, $v_1 = 0.1247$, $v_2 = 0.1944$ and $\alpha = 0.14725$. The resulting implied volatilities are plotted in Figure 5, where they are compared with the market mid volatilities.

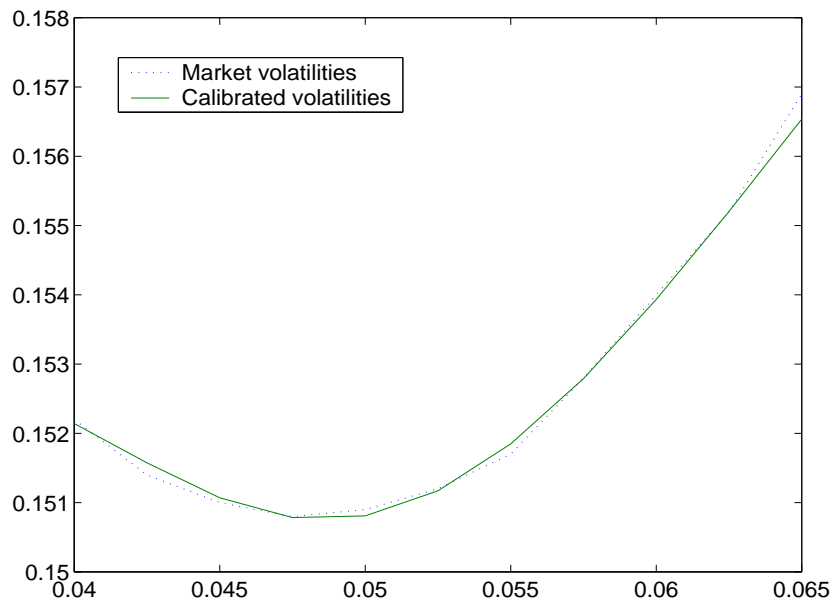


Figure 5: Plots of the calibrated volatilities vs the market mid volatilities.

In this example we could obtain a satisfactory fitting to the considered market data already with a mixture of two densities. Indeed, the fact that the implied volatility smile is almost flat helped in achieving such a calibration result. However, as also shown in Brigo and Mercurio (2000b), steeper curves may be well reproduced too. To this end, increasing the number N of basic lognormal densities may be helpful to retrieve a larger variety of implied volatility structures.

5.3 Calibration to a whole volatility surface: the EUR/USD rate case

We consider here a different case, namely that of the EUR/USD market volatility structure on May 17, 2001. The implied volatility surface as a function of time to maturity (T) and

option delta is reported in Fig. 6, upper part. It is customary in the FX market to quote volatilities in terms of three parameters per maturity: ATM volatility (σ_{ATM}), risk-reversal (r), strangle parameter (s). A thorough treatment of these types of options can be found in Malz (1997). Suffice it to say that a common assumption for a functional form that interpolates the observed market prices of vanilla options is

$$\sigma(\delta, T) = \sigma_{ATM}(T) - 2r(T) \left(\delta - \frac{1}{2} \right) + 16s(T) \left(\delta - \frac{1}{2} \right)^2, \quad (30)$$

with

$$\delta = e^{-r_d T} \Phi \left[\frac{\ln(S_t/X) + (r_d - r_f + \frac{\sigma^2}{2})(T - t)}{\sigma \sqrt{T - t}} \right] \quad (31)$$

being the delta of a call option. The relevant parameters (at-the-money volatility, risk-reversal and strangle) for the two dates at hand are quoted in Table 1, along with estimates of the bid/ask spread on the implied volatility on each maturity date. It is evident that

T	σ_{ATM}	r	s	Bid/ask spread
O/N	13.50%	0.60%	0.29 %	2%-2.5%
1W	10.50%	0.60%	0.29%	2%-2.5%
2W	10.40%	0.40%	0.29%	1%-1.5%
1M	11.00%	0.40%	0.30%	0.35%-0.85%
2M	11.15%	-0.05%	0.30%	0.30%-0.80%
3M	11.50%	-0.05%	0.30%	0.30%-0.80%
6M	11.85%	-0.10%	0.30%	0.30%-0.68%
9M	12.00%	-0.14%	0.30%	0.30%-0.55%
1Y	12.05%	-0.15%	0.30%	0.25%-0.45%
2Y	12.05%	-0.15%	0.30%	0.25%-0.45%

Table 1: Market data for ATM implied vols, risk-reversal and strangle prices as of May 17, 2001.

short maturity options (with maturities ranging from one week to two weeks) are not very liquid, a feature to be borne in mind when judging the results of calibration.

We have calibrated the model under the assumption of individual shifts depicted in Section 4.1, and explored the effect of varying the number of basis densities N . In order to accurately fit the market data, an appropriate choice for the integrated volatilities $\eta_i(T) = \sqrt{\frac{1}{T} \int_0^T \sigma_i^2(s) ds}$ of Eq. (16) must be made. We set

$$\eta^i(T) = \eta(T; a_i, b_i, c_i, \tau_i) = a_i + b_i \left[1 - \exp \left(-\frac{T}{\tau_i} \right) \right] \frac{\tau_i}{T} + c_i \exp \left(-\frac{T}{\tau_i} \right), \quad (32)$$

a functional dependence already proposed by Nelson and Siegel (1987) in the context of yield curve modelling. When calibrating the mixture of an n -component model, the vector

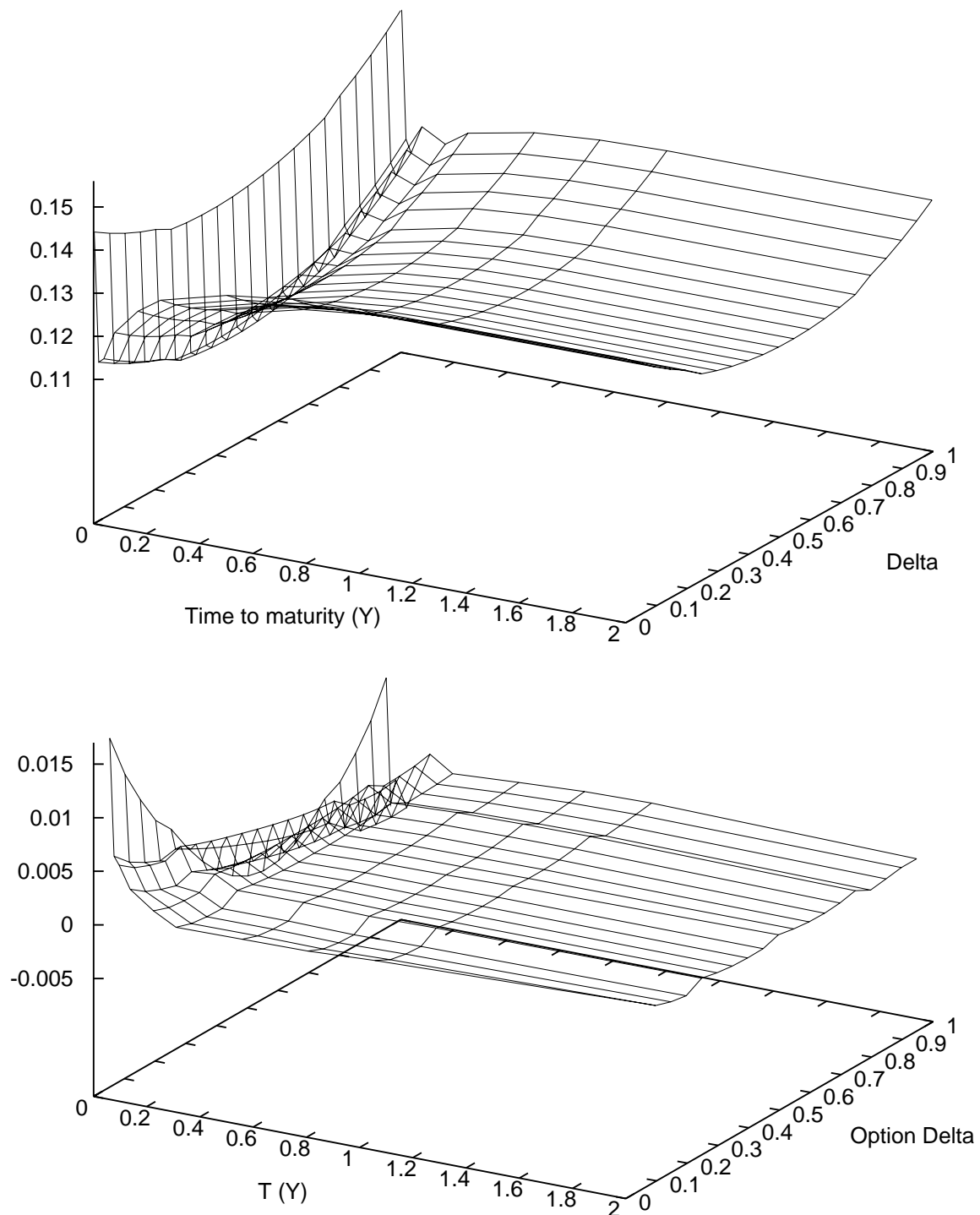


Figure 6: The market implied volatility surface (above) and absolute difference in implied volatility after calibration of the model with $N = 3$ (below) for the May 17, 2001 market data.

of optimization parameters $\mathbf{x} = (\lambda_1, \dots, \lambda_{n-1}, \beta_1, \dots, \beta_n, a_1, \dots, a_n, b_1, \dots, b_n, c_1, \dots, c_n, \tau_1, \dots, \tau_n)$ has dimensionality $4n + n + (n - 1) = 6n - 1$.

The calibration procedure consists in minimizing the function

$$F(\mathbf{x}) = \frac{1}{ML} \sum_{k=1}^M \sum_{j=1}^L \left(\frac{\Pi^{theo}(T_k, K_j; \mathbf{x}) - \Pi^{mkt}(T_k, K_j)}{\Pi^{mkt}(T_k, K_j)} \right)^2 \quad (33)$$

with respect to the parameter vector \mathbf{x} . Here $\Pi^{mkt}(T, K)$ denotes the mid market price of a European call option with maturity T and strike K , and $\Pi^{theo}(T, K; \mathbf{x})$ is the corresponding price given by the mixture of lognormal model for a choice of the parameter vector \mathbf{x} . This calibration differs from the former in that the model must now reproduce the volatility smile structure of vanilla options across all quoted maturities, from overnight to two years. The resulting root-mean-square error (square root of Eq. (33)) is 3×10^{-4} and 7×10^{-5} for calibrations based on two component and four component mixtures, respectively. A plot of the difference between the market implied volatility and the corresponding model volatility is given in Fig. 6, as a function of the option maturity (in years) and delta (which is indirectly related to the strike of the option through Eq. (31)). The maximum error for any maturity is well below the corresponding bid-ask spread of Table 1 already with only three components in the density.

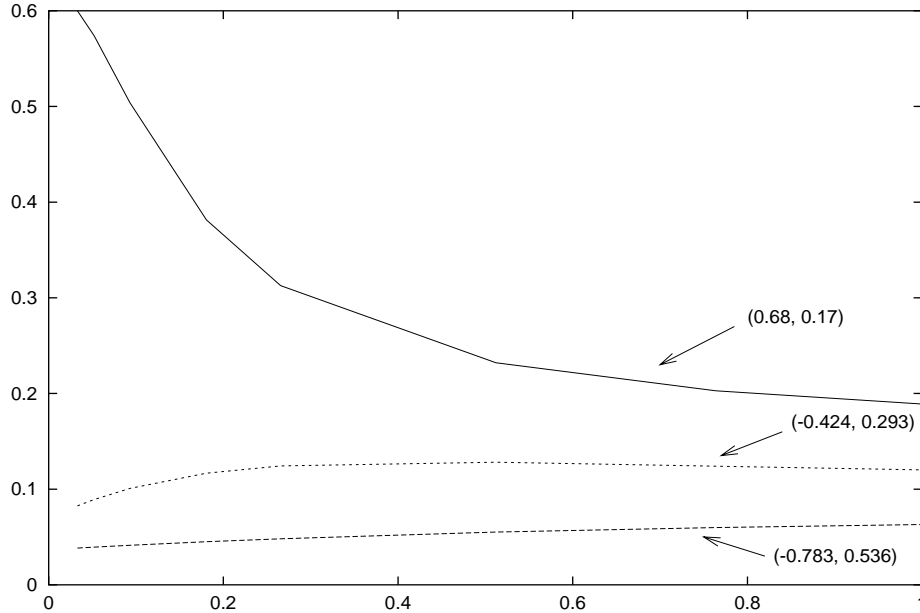


Figure 7: The integrated volatilities $\eta_i(T)$ of Eqs. (16) and (32) after calibration of the model with $N = 3$ on the May 17, 2001 market data. T is measured in years. Brackets enclose the shift and weight parameter: (β_i, λ_i) for each component.

In Fig. 7 we plot the $\eta_i(T)$ of Eq. (32) as functions of T measured in years from today.

Each curve in the picture is labeled with the corresponding β and λ (shift parameter and weight in the mixture, respectively). It is interesting to carefully examine the evolution of these functions when the number of components in the mixture varies: in Fig. 8 the two η_i only show a mild monotonic behaviour; adding a third component (Fig. 7) allows for a greater flexibility of the model in properly fitting the short maturity end of the implied volatility surface (usually the most difficult to reproduce) and this happens through a low-weight basis density (17% weight) with a rapidly decreasing $\eta(T)$. An additional component (see Fig. 9) does not change the general picture in a significant way.

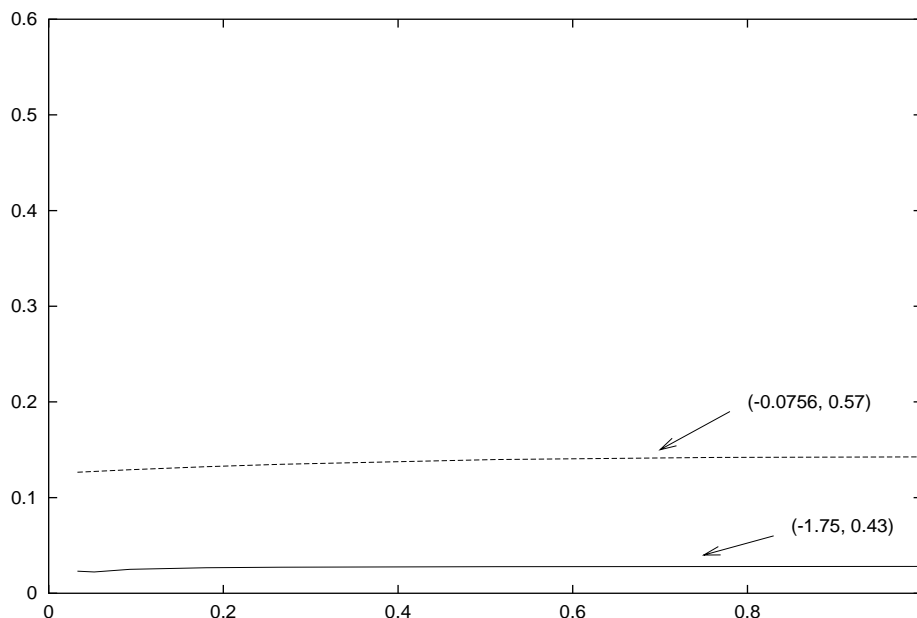


Figure 8: Same as in Fig. 7 with $N = 2$.

A final word should be spent on the density resulting from the mixture (Eq. (5)) when the number of component densities p_t^i varies. Careful inspection of Fig. 10 shows a process of convergence of the resulting density (plotted for a one year horizon) as the number of components is increased from one to four.

6 Conclusions

We have proposed asset-price models capable of reproducing quite general volatility structures. First we have introduced and explained the “lognormal-mixture” asset-price dynamics, and then we have extended this model by means of general transformations. All models are analytically tractable, and explicit prices for European-style call options are readily derived as linear combinations of Black-Scholes prices.

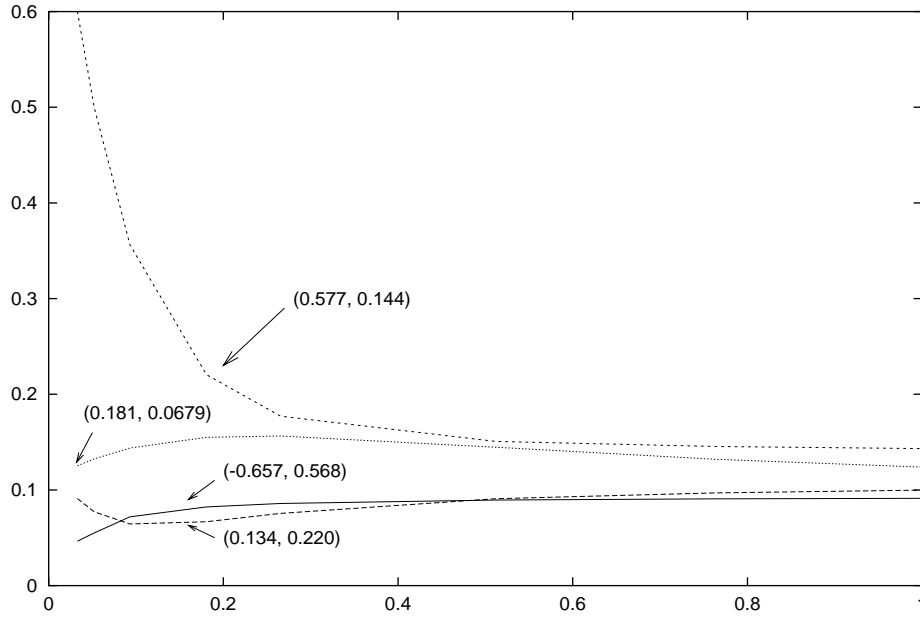


Figure 9: Same as in Fig. 7 with $N = 4$.

Furthermore, once calibrated to the plain vanilla market, any of these models allows to price exotic path-dependent claims through Monte Carlo simulation.

Very few existing models propose explicit asset-price dynamics that are consistent with a given risk-neutral (forward) distribution. Moreover, the arbitrarily large number and controllability of parameters render our model unique from this point of view. In fact, choosing as many parameters as we like produces a large flexibility in the model calibration to real option data, although one needs to beware of possible problems related to overfitting and feasibility of the calibration process as far as the execution time is concerned.

Appendix

In this appendix, we calculate the skewness and kurtosis of the marginal distribution of the log-process $\bar{S}_t := \ln(S_t)/\ln(S_0)$, $t > 0$. As is easily shown, for each $t > 0$ the density of \bar{S}_t is given by the mixture of normal densities:

$$\begin{aligned}
 \bar{p}_t(y) &:= \frac{d}{dy} Q^T \left\{ \ln \frac{S_t}{S_0} \leq y \right\} \\
 &= S_0 e^y p_t(S_0 e^y) \\
 &= \sum_{i=1}^N \lambda_i \frac{1}{V_i(t) \sqrt{2\pi}} \exp \left\{ -\frac{1}{2V_i^2(t)} \left[y - \mu t + \frac{1}{2} V_i^2(t) \right]^2 \right\}.
 \end{aligned}$$

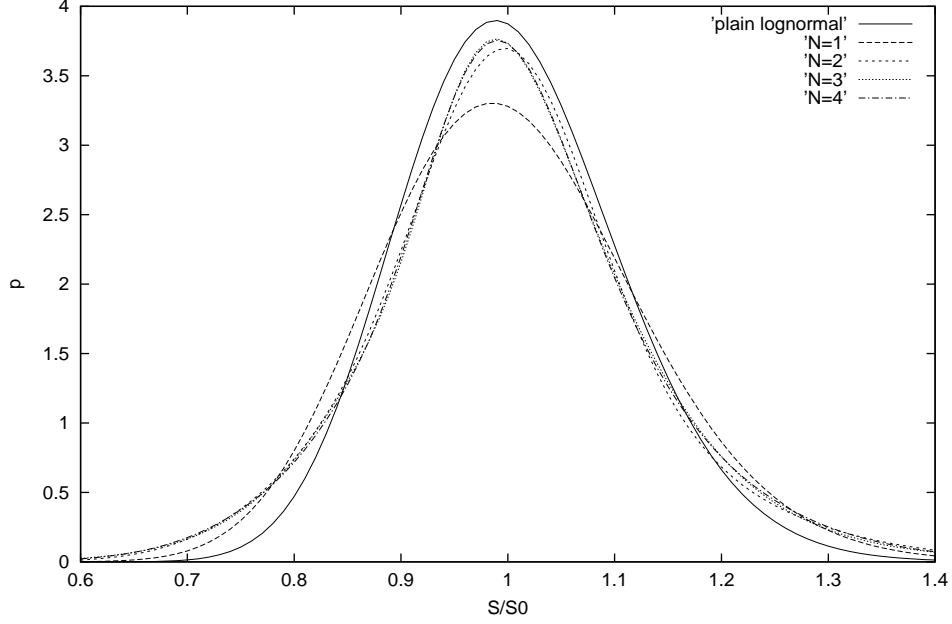


Figure 10: The probability densities resulting from the mixture after calibration of the model on the May 17, 2001 market data, for varying numbers N of basis densities of Eq. (5). The solid line represents a single (non shifted) lognormal process density calibrated to the whole implied volatility surface, the other lines refer to the shifted basis densities for $N = 1, \dots, 4$, as described in the legenda.

Using the fact that every (central) moment of a linear combination of densities is given by the (same) linear combinations of the corresponding moments, we have:

$$\begin{aligned}
E^T\{\bar{S}_t\} &= \mu t - \frac{1}{2}\mathcal{V}_2(t), \\
E^T\{\bar{S}_t^2\} &= \mu^2 t^2 + (1 - \mu t)\mathcal{V}_2(t) + \frac{1}{4}\mathcal{V}_4(t), \\
E^T\{\bar{S}_t^3\} &= \mu^3 t^3 + 3\mu t\left(1 - \frac{1}{2}\mu t\right)\mathcal{V}_2(t) + \frac{3}{4}(\mu t - 2)\mathcal{V}_4(t) - \frac{1}{8}\mathcal{V}_6(t), \\
E^T\{\bar{S}_t^4\} &= \mu^4 t^4 - 2\mu^2 t^2(\mu t - 3)\mathcal{V}_2(t) + \frac{3}{2}\left(\mu^2 t^2 - 4\mu t + 2\right)\mathcal{V}_4(t) - \frac{1}{2}(\mu t - 3)\mathcal{V}_6(t) + \frac{1}{16}\mathcal{V}_8(t),
\end{aligned}$$

where

$$\mathcal{V}_k(t) := \sum_{i=1}^N \lambda_i V_i^k(t).$$

Tedious but straightforward calculations lead to the following expressions for the variance, skewness and kurtosis of \bar{S}_t under Q^T :

$$\begin{aligned}\text{Var}^T\{\bar{S}_t\} &= \mathcal{V}_2(t) + \frac{1}{4}\mathcal{V}_4(t) - \frac{1}{4}(\mathcal{V}_2(t))^2 \\ \text{Skew}^T\{\bar{S}_t\} &= \frac{12(\mathcal{V}_2(t))^2 - 2(\mathcal{V}_2(t))^3 + 3\mathcal{V}_2(t)\mathcal{V}_4(t) - 12\mathcal{V}_4(t) - \mathcal{V}_6(t)}{8\left(\mathcal{V}_2(t) + \frac{1}{4}\mathcal{V}_4(t) - \frac{1}{4}(\mathcal{V}_2(t))^2\right)^{3/2}} \\ \text{Kurt}^T\{\bar{S}_t\} &= \frac{48\mathcal{V}_4(t) + 24\mathcal{V}_6(t) + 24(\mathcal{V}_2(t))^3 - 48\mathcal{V}_2(t)\mathcal{V}_4(t)}{16\left(\mathcal{V}_2(t) + \frac{1}{4}\mathcal{V}_4(t) - \frac{1}{4}(\mathcal{V}_2(t))^2\right)^2} \\ &\quad + \frac{\mathcal{V}_8(t) + 6(\mathcal{V}_2(t))^2\mathcal{V}_4(t) - 3(\mathcal{V}_2(t))^4 - 4\mathcal{V}_2(t)\mathcal{V}_6(t)}{16\left(\mathcal{V}_2(t) + \frac{1}{4}\mathcal{V}_4(t) - \frac{1}{4}(\mathcal{V}_2(t))^2\right)^2}\end{aligned}$$

The above expressions are rather involved and difficult to study. Indeed, it may be helpful to rearrange them as follows:

$$\begin{aligned}\text{Var}^T\{\bar{S}_t\} &= \sum_{i=1}^N \lambda_i V_i^2(t) + \frac{1}{4} \sum_{i=1}^N \lambda_i \left[V_i^2(t) - \sum_{j=1}^N \lambda_j V_j^2(t) \right]^2 \\ \text{Skew}^T\{\bar{S}_t\} &= - \frac{12 \sum_{i=1}^N \lambda_i \left(V_i^2(t) - \sum_{j=1}^N \lambda_j V_j^2(t) \right)^2 + \sum_{i=1}^N \lambda_i \left(V_i^2(t) - \sum_{j=1}^N \lambda_j V_j^2(t) \right)^3}{8 \left[\sum_{i=1}^N \lambda_i V_i^2(t) + \frac{1}{4} \sum_{i=1}^N \lambda_i \left(V_i^2(t) - \sum_{j=1}^N \lambda_j V_j^2(t) \right)^2 \right]^{3/2}} \\ &= - \frac{\sum_{i=1}^N \lambda_i \left(V_i^2(t) - \sum_{j=1}^N \lambda_j V_j^2(t) \right)^2 \left(12 + V_i^2(t) - \sum_{j=1}^N \lambda_j V_j^2(t) \right)}{8 \left[\sum_{i=1}^N \lambda_i V_i^2(t) + \frac{1}{4} \sum_{i=1}^N \lambda_i \left(V_i^2(t) - \sum_{j=1}^N \lambda_j V_j^2(t) \right)^2 \right]^{3/2}} \\ \text{Kurt}^T\{\bar{S}_t\} &= \frac{48 \sum_{i=1}^N \lambda_i V_i^4(t) + 24 \sum_{i=1}^N \lambda_i V_i^2(t) \left(V_i^2(t) - \sum_{j=1}^N \lambda_j V_j^2(t) \right)^2}{16 \left[\sum_{i=1}^N \lambda_i V_i^2(t) + \frac{1}{4} \sum_{i=1}^N \lambda_i \left(V_i^2(t) - \sum_{j=1}^N \lambda_j V_j^2(t) \right)^2 \right]^2} \\ &\quad + \frac{\sum_{i=1}^N \lambda_i \left(V_i^2(t) - \sum_{j=1}^N \lambda_j V_j^2(t) \right)^4}{16 \left[\sum_{i=1}^N \lambda_i V_i^2(t) + \frac{1}{4} \sum_{i=1}^N \lambda_i \left(V_i^2(t) - \sum_{j=1}^N \lambda_j V_j^2(t) \right)^2 \right]^2} \\ &= 3 + \frac{\sum_{i=1}^N \lambda_i \left(V_i^2(t) - \sum_{j=1}^N \lambda_j V_j^2(t) \right)^2 \left[48 + 24U_i + U_i^2 - 3 \sum_{j=1}^N \lambda_j U_j^2 \right]}{16 \left[\sum_{i=1}^N \lambda_i V_i^2(t) + \frac{1}{4} \sum_{i=1}^N \lambda_i \left(V_i^2(t) - \sum_{j=1}^N \lambda_j V_j^2(t) \right)^2 \right]^2},\end{aligned}$$

where, in the last step, we have set $U_i := V_i^2(t) - \sum_{k=1}^N \lambda_k V_k^2(t)$.

We can easily see that a sufficient condition for the skewness to be negative is that $12 + V_i^2(t) - \sum_{j=1}^N \lambda_j V_j^2(t) \geq 0$ for each i , whereas a sufficient condition for the kurtosis to be larger than 3 is that $48 + 24U_i + U_i^2 - 3 \sum_{j=1}^N \lambda_j U_j^2 \geq 0$ for each i . Indeed such conditions are largely satisfied for realistic (non-pathological) values of the model parameters.

In order to deal with more user-friendly expressions, we can neglect all terms with $V_1^\alpha(t)V_2^\beta(t)$ of non-minimum degree, which leads to the following approximations:

$$\begin{aligned}\text{Var}^T\{\bar{S}_t\} &\approx \mathcal{V}_2(t) = \sum_{i=1}^N \lambda_i V_i^2(t) \\ \text{Skew}^T\{\bar{S}_t\} &\approx \frac{3}{2} \frac{(\mathcal{V}_2(t))^2 - \mathcal{V}_4(t)}{(\mathcal{V}_2(t))^{3/2}} = -\frac{3}{2} \frac{\sum_{i=1}^N \lambda_i \left(V_i^2(t) - \sum_{j=1}^N \lambda_j V_j^2(t)\right)^2}{\left(\sum_{i=1}^N \lambda_i V_i^2(t)\right)^{3/2}} \leq 0 \\ \text{Kurt}^T\{\bar{S}_t\} &\approx 3 \frac{\mathcal{V}_4(t)}{(\mathcal{V}_2(t))^2} = 3 + 3 \frac{\sum_{i=1}^N \lambda_i \left(V_i^2(t) - \sum_{j=1}^N \lambda_j V_j^2(t)\right)^2}{\left(\sum_{i=1}^N \lambda_i V_i^2(t)\right)^2} \geq 3\end{aligned}$$

Such approximations turn out to be accurate in most practical situations, and especially for non-pathological values of the model parameters.

As an example, we finally consider the particular case of a mixture of two densities, and set, therefore, $N = 2$, $\lambda_1 := \lambda$ and $\lambda_2 := 1 - \lambda$. We obtain:

$$\begin{aligned}\text{Var}^T\{\bar{S}_t\} &\approx \lambda V_1^2(t) + (1 - \lambda)V_2^2(t) \\ \text{Skew}^T\{\bar{S}_t\} &\approx -\frac{3}{2} \frac{\lambda(1 - \lambda)(V_1^2(t) - V_2^2(t))^2}{(\lambda V_1^2(t) + (1 - \lambda)V_2^2(t))^{3/2}} \\ \text{Kurt}^T\{\bar{S}_t\} &\approx 3 \frac{\lambda V_1^4(t) + (1 - \lambda)V_2^4(t)}{(\lambda V_1^2(t) + (1 - \lambda)V_2^2(t))^2}\end{aligned}$$

from which it is immediate that, for given $V_1(t)$ and $V_2(t)$, $\text{Kurt}^T\{\bar{S}_t\}$ is maximum for

$$\lambda = \lambda^* := \frac{V_2^2(t)}{V_1^2(t) + V_2^2(t)}$$

and the value of the maximum kurtosis is

$$\text{Kurt}^T\{\bar{S}_t\}|_{\lambda=\lambda^*} = \frac{(V_1^2(t) + V_2^2(t))^2}{4V_1^2(t)V_2^2(t)}.$$

Letting $V_1(t)$ and $V_2(t)$ vary as well, the maximum kurtosis can grow indefinitely (to infinity).

References

- [1] Avellaneda, M., Friedman, C., Holmes, R. and Samperi D. (1997) Calibrating Volatility Surfaces via Relative-Entropy Minimization. Preprint. Courant Institute of Mathematical Sciences. New York University.
- [2] Black, F. and Scholes, M. (1973) The Pricing of Options and Corporate Liabilities. *Journal of Political Economy* 81, 637-659.
- [3] Bhupinder, B. (1998) Implied Risk-Neutral Probability Density Functions from Option Prices: A Central Bank Perspective. In *Forecasting Volatility in the Financial Markets*, 137-167. Edited by Knight, J., and Satchell, S. Butterworth Heinemann. Oxford.
- [4] Breeden, D.T. and Litzenberger, R.H. (1978) Prices of State-Contingent Claims Implicit in Option Prices. *Journal of Business* 51, 621-651.
- [5] Brigo, D., and Mercurio, F. (2000a). Analytical models for volatility smiles and skews. Banca IMI internal report.
- [6] Brigo, D., and Mercurio, F. (2000b). A mixed-up smile. *Risk* September, 123-126.
- [7] Britten-Jones, M. and Neuberger, A. (1999) Option Prices, Implied Price Processes and Stochastic Volatility. Preprint. London Business School.
- [8] Carr, P., Tari, M. and Zariphopoulou T. (1999) Closed Form Option Valuation with Smiles. Preprint. NationsBanc Montgomery Securities.
- [9] Cox, J. (1975) Notes on Option Pricing I: Constant Elasticity of Variance Diffusions. Working paper. Stanford University.
- [10] Cox, J. and Ross S. (1976) The Valuation of Options for Alternative Stochastic Processes. *Journal of Financial Economics* 3, 145-166.
- [11] Derman, E. and Kani, I. (1994) Riding on a Smile. *Risk* February, 32-39.
- [12] Derman, E. and Kani, I. (1998) Stochastic Implied Trees: Arbitrage Pricing with Stochastic Term and Strike Structure of Volatility. *International Journal of Theoretical and Applied Finance* 1, 61-110.
- [13] Dupire, B. (1994) Pricing with a Smile. *Risk* January, 18-20.
- [14] Dupire, B. (1997) Pricing and Hedging with Smiles. *Mathematics of Derivative Securities*, edited by M.A.H. Dempster and S.R. Pliska, Cambridge University Press, Cambridge, 103-111.
- [15] Guo, C. (1998) Option Pricing with Heterogeneous Expectations. *The Financial Review* 33, 81-92.

- [16] Heston, S. (1993) A Closed Form Solution for Options with Stochastic Volatility with Applications to Bond and Currency Options. *Review of Financial Studies* 6, 327-343.
- [17] Hull, J. and White, A. (1987) The Pricing of Options on Assets with Stochastic Volatilities. *Journal of Financial and Quantitative Analysis* 3, 281-300.
- [18] Jackwerth, J.C. and Rubinstein, M. (1996) Recovering Probability Distributions from Option Prices. *Journal of Finance* 51, 1611-1631.
- [19] Melick, W.R., and Thomas, C.P. (1997) Recovering an Asset's Implied PDF from Option Prices: An Application to Crude Oil During the Gulf Crisis. *Journal of Financial and Quantitative Analysis* 32, 91-115.
- [20] Musiela, M. and Rutkowski, M. (1998) *Martingale Methods in Financial Modelling*. Springer. Berlin.
- [21] Nelson, C.R., and Siegel, A.F. (1987) Parsimonious Modeling of Yield Curves, *Journal of Business* 60, 473-489.
- [22] Prigent, J.L., Renault O. and Scaillet O. (2000) An Autoregressive Conditional Binomial Option Pricing Model. Preprint. Université de Cergy.
- [23] Ritchey, R.J. (1990) Call Option Valuation for Discrete Normal Mixtures. *Journal of Financial Research* 13, 285-296.
- [24] Rubinstein, M. (1994) Implied Binomial Trees. *Journal of Finance* 49, 771-818.
- [25] Shimko, D. (1993) Bounds of Probability. *Risk* April, 33-37.
- [26] Tompkins, R.G. (2000a) Stock Index Futures Markets: Stochastic Volatility Models and Smiles. Preprint. Department of Finance. Vienna University of Technology.
- [27] Tompkins, R.G. (2000b) Fixed Income Futures Markets: Stochastic Volatility Models and Smiles. Preprint. Department of Finance. Vienna University of Technology.